Journal of Low Temperature Physics, Vol. 87, Nos. 5/6, 1992

Determination of the Electric Field Gradient and Relaxation Time Measurements in Scandium Metal at Very Low Temperature

L. Pollack, E. N. Smith, J. M. Parpia, and R. C. Richardson

Cornell Microkelvin Laboratory, Materials Science Center, Cornell University, Ithaca, New York

(Received November 12, 1991; revised January 2, 1992)

We present the results of measurements on a single crystal sample of scandium metal at temperatures down to 100 μK using nuclear quadrupole resonance (NQR). We find two regimes in the relaxation curves: an initial fast relaxation, followed by a slower relaxation consistent with the three exponential recovery expected for an $I = 7/2$ system in zero external magnetic field. The Korringa constant for this longer time relaxation in our sample is 90 ± 9 msec K^{-1}. By observing deviations in the ratio of the intensities of adjacent nuclear spin transitions at the lowest attainable temperatures, we have been able to make a determination of the sign of the total electric field gradient present in the crystal. We find that the lowest energy state of the nuclear spin system corresponds to $m_I = \pm 7/2$. A combination of these deviations and pulse NQR allows us to use this system as an absolute thermometer in the μKelvin regime.

1. INTRODUCTION

Quadrupolar systems present several unique opportunities for study at very low temperatures. The origin of the splitting of the nuclear energy levels is the interaction of the electric quadrupole moment of the nucleus with the electric field gradient present at the nucleus. It is therefore possible to make measurements at zero external magnetic field. We have measured spin-lattice relaxation times in single crystal samples of pure scandium (Sc) metal at zero field over a temperature range from 300 μK to 10 mK. The model for relaxation based on mutual nuclear-electron spin flips[1-3] predicts a multi-exponential decay for pure quadrupolar systems. We find two separate regimes in the relaxation curves. At short times ($t \ll 1$ sec) after saturation a very fast relaxation is observed. Relaxation curves compatible with a three-exponential decay are measured at all temperatures for times greater than 1 sec after saturation. The value of the Korringa constant that

0022-2291/92/0600-0753$06.50/0

we obtain from this long time relaxation is an order of magnitude smaller than the value measured at high temperature and high field along the c-axis.[4] The zero field value is expected to be a factor of 2 smaller than the high field value if the nuclear spin coupling is strictly dipolar;[1,5] however, in experiments performed elsewhere larger reductions of the Korringa constant have been observed in some samples of Cu[6] and Pt[7] at low temperature and low field.

After determining the spin-lattice relaxation times we have also demonstrated the use of these systems as absolute thermometers by simultaneous measurements of the population differences in two adjacent transitions as a function of temperature. In the infinite temperature limit, where the characteristic splitting of the energy levels $\Delta E \ll kT$, the ratio of the intensity in the two transitions is constant. As the temperature is decreased the ratio of intensity of the higher frequency transition to that of the lower frequency transition increases. Once the high temperature value is measured, a given value of the ratio corresponds to a unique and calculable value of temperature.

From these measurements we have also made the first determination of the sign of the total electric field gradient in Sc. We find that the lowest energy state corresponds to $m_I = \pm 7/2$. This information, combined with the expected value of the lattice contribution to the internal electric field gradient[8] suggests that the field gradient from the non-s nature of the conduction electrons has the same sign as the contribution from the lattice and is about the same size.

2. BACKGROUND

2.1. Quadrupolar Interactions

The coupling of the nuclear electric quadrupole moment to the lattice can be observed under the following conditions. The nuclear spin, I, must be greater than $1/2$ since the interaction depends on the orientation of the nucleus. An electric field gradient must also be present in the crystal.[9] In the simplest case of an axially symmetric field gradient the energy levels in zero external magnetic field are described by

$$E_{m_I} = \frac{e^2qQ}{4I(2I-1)}(3m_I^2 - I(I+1)) \tag{1}$$

In this expression eQ is the electric quadrupole moment of the nucleus, and eq is the total electric field gradient present at the nucleus. From this expression it is clear that the $\pm m_I$ levels are degenerate and that the energy levels are not equally spaced (see Fig. 1). This feature is critical to all of the measurements reported in this paper.

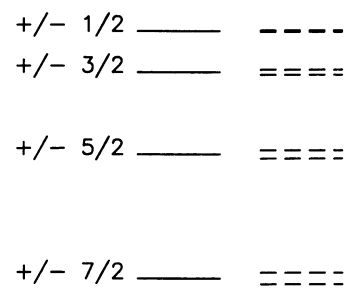

Fig. 1. The energy levels of an $I=7/2$ nucleus are shown in the case of pure quadrupolar splitting on the left, and in the presence of a small magnetic field on the right. Note that in the pure case, the $\pm m_I$ levels are degenerate.

For Sc the energy levels are described by Eq. (1) with $e^2qQ/h =$ 2.0 MHz, where $Q=-0.22$ barns[10] and $I=7/2$. The size of the splittings in Sc are 130 kHz between the $\pm 1/2$ and the $\pm 3/2$ states; 260 kHz between the $\pm 3/2$ and the $\pm 5/2$ states and 390 kHz between the $\pm 5/2$ and the $\pm 7/2$ states. In temperature these splittings correspond to 6, 12, and 18 μK. The sign of q, the gradient, will determine whether the $\pm 7/2$ states or the $\pm 1/2$ states have the lowest energy at zero field.

If the crystal is non-cubic there are two contributions to the gradient. The first is associated with the lattice of ion cores. This part of the gradient is calculable for an hcp crystal[11] if the c/a ratio and the Sternheimer anti-shielding factor[12] are known. The second contribution to the gradient is the non-s nature of the conduction electrons which is difficult to calculate since it depends on the details of the band structure of the crystal. Since the gradient is assumed to be the sum of these two, the conduction electron component can be inferred from a measurement of the total gradient. For the case of nuclei which do not have a radioactive isotope,[13] determination of this sign requires cooling the sample down to a temperature which is of the order of the characteristic level spacing and measuring either the heat capacity[14] or the relative population in different levels. For Sc this requires cooling the system to a temperature on the order of 100 μK since the condition $\Delta E \ll kT$ starts to break down in this regime.

2.2. NQR

Population differences between the different m_I levels can be measured with pulse techniques, similar to pulse NMR. Either free induction decays (FID)[15] or spin-echoes[16] can be observed. In the case of pure quadrupolar splitting (zero external field) there is no net nuclear magnetization since the $\pm m_I$ levels are degenerate. The excitation and pickup coils must not have orthogonal axes and the signal results from the constructive interference of the $\pm m_I$ components as they precess in opposite directions after a tipping pulse.[15] It is common to use the same coil for both purposes.

Generation of an FID is preferable since this method measures the population differences immediately before the pulse is applied, thus one need not worry about the possibility of eddy-current heating of the system from the pulse.[17] It is advantageous to use a single crystal for these measurements since the gradients will be more uniform than in a poly-crystalline sample. In the current studies on single crystal samples FIDs are clearly visible up to 8 mK. In our previous studies on the polycrystalline samples[18] of similar size, FIDs were only visible below 1 mK due to inhomogeneity of the gradients. Since the spin-spin relaxation time of the sample is short the spin-echo technique makes it possible to take data at higher temperatures. As a check we can compare the value of T_1 obtained by both techniques at a suitably low temperature. We find good agreement between the two methods. Therefore the spin-echo technique may be used to examine relaxation at higher temperatures where the signals are smaller, but heating effects are not expected to be a concern.

2.3. Relaxation Times

At low temperature the relaxation time T_1 is a measure of the nuclear spin-conduction electron coupling since the lattice degrees of freedom are frozen out. In the NQR case, where the levels are unequally spaced, mutual nuclear spin flips do not always conserve both energy and angular momentum. Therefore during the relaxation process the nuclear spin levels are not at a unique spin temperature. Each level has a characteristic time constant with which it relaxes to the lattice temperature. Eventually, after relaxation is complete, the nuclear spin temperature is equal to the lattice temperature. However, changing the population in one level can affect the population differences in more than one set of levels. For instance if the 3/2 to 5/2 level is saturated it is clear that all of the population differences will be altered from their equilibrium values. For the case of magnetic ($\Delta m = 1$) transitions in an $I = 7/2$ system the time dependent return to equilibrium of the population difference between adjacent levels after an initial disturbance can be derived from basic quantum mechanics[3] and has the form

$$M_{eq} - M(t) = A \exp\left(\frac{-3t}{T_1}\right) + B \exp\left(\frac{-10t}{T_1}\right) + C \exp\left(\frac{-21t}{T_1}\right) \qquad (2)$$

In this expression A, B, and C are constants that depend on the initial spin conditions and T_1 is the corresponding magnetic relaxation time. At higher temperatures $\Delta m = 2$ transitions which are mediated by the lattice can occur;[19] however, at the low temperatures of this work only $\Delta m = 1$ transitions are expected. The most important features of this equation are the effective time constants which are well defined fractions of T_1; consequently the relaxation is faster than in a comparable magnetically split system.

2.4. Thermometry

Quadrupolar systems have important applications as absolute thermometers at low temperatures. The relevant temperature range is dictated by the characteristic splitting of the levels. In a system which has two unequally spaced transitions of energies ε_1 and ε_2 the ratios of the relative populations of the levels change in a unique way with temperature. The following general expression results for the ratio of population in the higher energy transition to that in the lower energy transition

$$R = \exp\frac{(\varepsilon_1+\varepsilon_2)}{2kT}\,\frac{\sinh(\varepsilon_1/2kT)}{\sinh(\varepsilon_2/2kT)} \tag{3}$$

In this expression k is the Boltzmann constant. When the ambient temperature $T \gg \varepsilon_1/k$, ε_2/k, Eq. (3) reduces to $R = \varepsilon_1/\varepsilon_2$ and is independent of temperature. In the regime where Eq. (3) can be used a given value of R corresponds to a unique value of T. The thermometer is calibrated by measuring the high temperature value of the ratio and normalizing the theory to that value. Figure 2 shows the expected behavior of R for the two highest frequency transitions.

A similar technique for creating an absolute thermometer based on applying a small magnetic field to a quadrupolar system and looking at the population differences between the Zeeman split levels has been proposed by Sullivan.[20]

3. APPARATUS

These measurements were made on a nuclear demagnetization cryostat consisting of an Oxford[21] model 600 dilution refrigerator and an 80 mole copper bundle. The sample is a single crystal foil of Sc metal obtained from Ames Labs.[22] The c-axis of the crystal is perpendicular to the plane of the foil. The foil size is 10 mm × 30 mm. Its thickness is tapered so that the upper part of the sample, where the pickup coil is mounted, has been electropolished to a thickness of 250 μm. This thickness is less than twice the skin depth at 260 kHz. At the bottom of the crystal, where it is thermally and mechanically anchored with a copper clamp, it is 500 μm thick. The electrical resistance of similar clamp joints has been measured to be on the order of $\mu\Omega$s. The sample is clamped onto a copper cone which is secured in a mating tapered hole on the stage plate of the cryostat. Compensation coils on the demagnetization magnet reduce the field in this vicinity to about 10 mT even when the main field is at 9 T. These small residual fields are screened from the sample by a superconducting Nb tube maintained at the temperature of the dilution refrigerator mixing chamber.

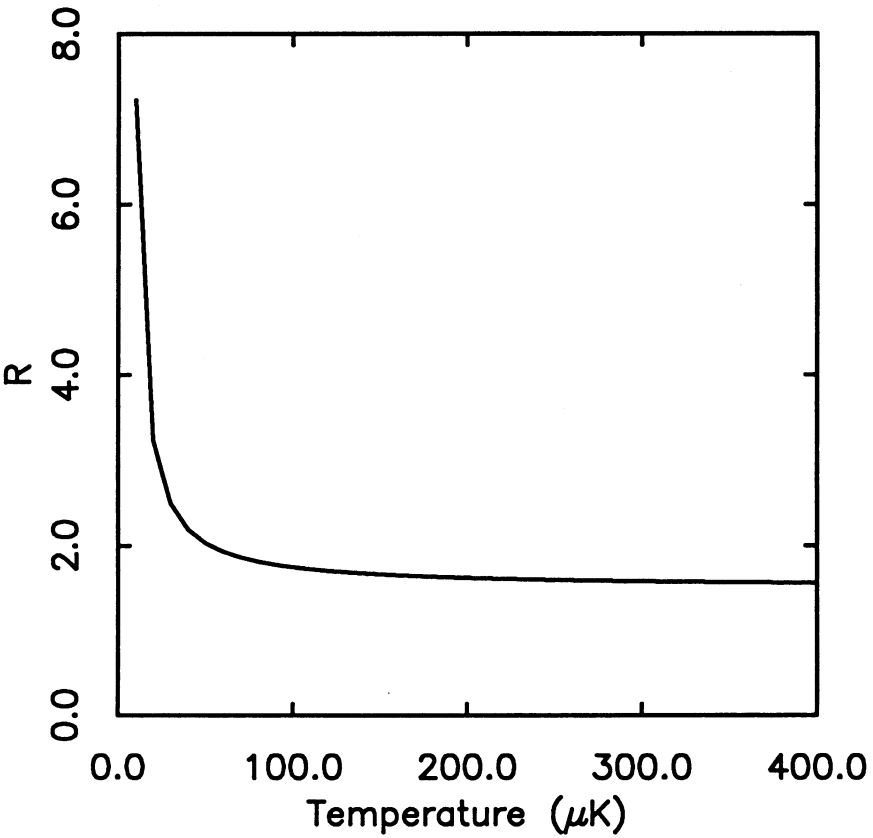

Fig. 2. A graph of the expected behavior of Eq. (3) as a function of temperature for the two higher frequency transitions.

A single excitation/pickup coil is used for the NQR experiments. It has an inductance of about 800 μH and is connected to the room temperature electronics by a superconducting cable. The natural resonance frequency of the circuit is 440 kHz; it can easily be tuned to any lower frequency by the addition of appropriate parallel capacitors at room temperature. It is possible to change the tuning on the μsec time scale by computer so that more than one transition can be studied; however, for the purpose of this work the tuning was kept fixed for a given experiment.

A diagram of the spectrometer used for all of the measurements is shown in Fig. 3. The entire system is controlled by the computer which is programmed to select appropriate sequences for the timing simulator, to adjust the frequency of the synthesizer, to initiate pulse sequences at the

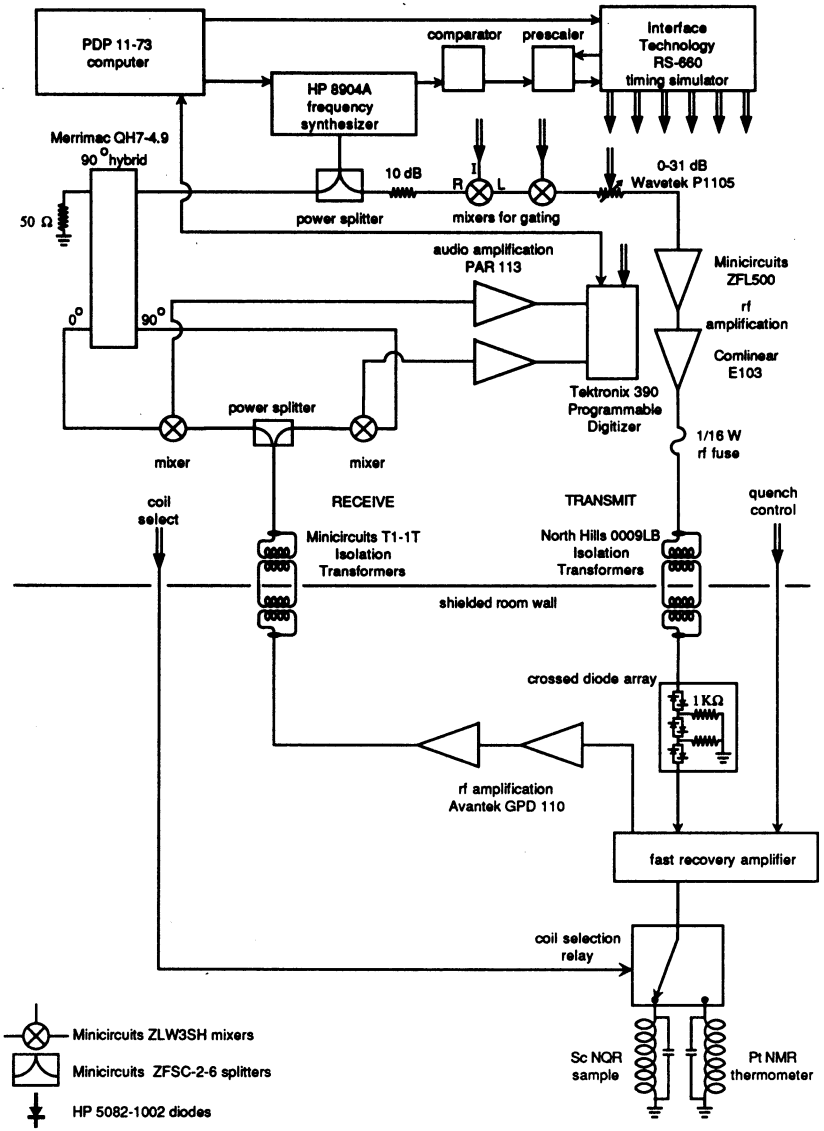

Fig. 3. A schematic diagram of the spectrometer electronics is shown. More information about the manufacturers is given in Ref. 23.

appropriate time intervals, and to record and do preliminary analysis on the data. One output from the synthesizer is converted into square wave and serves as an external clock for the timing simulator. The frequency of this external clock can be scaled by a logic circuit during portions of the timing sequence to allow us to make the very long (≈minutes) time scale measurements required for some of the T_1 measurements. A second output, phase shifted to obtain optimal pulse shape, provides rf input to the transmitter and detection circuits. Gating of the pulses in the transmitter circuit is achieved by using two mixers in series as a switch. This scheme achieves a better on/off ratio (>100 dB) than that from a single mixer, and a particularly clean pulse is generated (no excess ringing) when the first mixer is turned on for a longer time than the second by one rf cycle before and after. The amplitude of the transmitter pulse can then be adjusted by the computer controlled variable attenuator. We have determined that the best performance (little or no distortion of a pulse) occurs when using two lower power amplifiers in the transmitter. Once amplified, the pulse is fed through the wall of the shielded room through a series of high power isolation transformers and EMI filters. Several pairs of crossed diodes provide additional isolation of low level signals from the transmitter to the sample. Through the use of a logic circuit which is optically coupled to the electronics outside of the shielded room, an rf relay connects the selected coil. From room temperature to 4.2 K the coaxial cable is commercial Be-Cu hardline. Further down in the cryostat we use homemade superconducting coaxial cable. The spectrometer can generate pulses with peak to peak voltages of 15 V at the top of the cryostat.

The first stage of amplification on the receiver is a home-built preamplifier[24] which is mounted on the top plate of the cryostat at room temperature and sits inside the shielded room. The noise figure for this amplifier is $4\,\text{nV}/\sqrt{\text{Hz}}$. The use of an internal quench circuit reduces the dead time of the system to about 30 μsec. The control circuit for the quench circuit is located outside of the shielded room and optically isolated signals are transmitted through the wall. After amplification by the second stage of gain, the response of the spins is fed back through lower power isolation transformers and EMI filters to the outside of the shielded room. The signal is split and mixed with 0 and 90° reference signals before being amplified, filtered, and finally digitized and sent to the data acquisition computer.

The spectrometer is also used to monitor a ^{195}Pt NMR thermometer. All of the quoted temperatures are derived from the Pt susceptibility assuming a strict Curie law behavior. The Pt thermometer is calibrated using the Korringa relation (assuming $T_1 T = 29.6\,\text{msec K}^{-1}$) at dilution refrigerator temperature, typically 6–10 mK, and by checking against the "A" and solid transitions of the ^{3}He melting curve thermometer.[25] The field at which the

Pt NMR is measured is higher than any at which deviations from the above value of the Korringa constant have been observed (≈ 200 G).[7] The thermometer consists of 1000 turns of 5 N Pt wire from California Fine Wire Co.[26] TIG welded into a Pt rod. This rod is TIG welded into a silver post which is in turn TIG welded into a copper cone. The design is similar to that discussed in Ref. 7. The cone is attached to the stage plate in the same manner as that of the Sc experiment.

4. MEASUREMENTS

There are two types of measurements that are reported in this paper: those associated with the relaxation times and those associated with absolute thermometry. In this section we will discuss the experimental technique involved in making both kinds of measurements.

4.1. Relaxation Times

The relaxation time measurements are made by sampling the magnetization at time intervals ranging from hundreds of μsecs to hundreds of seconds after saturating the spins with a "comb" of between 50 and 75 pulses. The pulses in the comb are approximately 7° in tipping angle and are separated by a time longer than the inverse linewidth of the resonance line and significantly shorter than the expected value of T_1. A comb is required to saturate the sample. No magnetization is visible immediately after the comb. The sampling pulse is a single pulse of about 10° tipping angle so all of the relaxation measurements are based on FID signals. As a check on heating, every fourth sequence consists of a sampling pulse alone. The amplitude of the resulting FID is checked against the expected signal height at a given temperature. In this way we are confident that the ambient temperature of the cryostat does not change during the time interval required for a T_1 measurement. The thermal time constant of the clamp joint through which the electrons in the sample are cooled to the stage temperature is several orders of magnitude shorter than the measured value of T_1; therefore we do not expect to have significant heating from the pulsing on the time scale over which the experiments are done.

Different combinations of pulse duration in the comb, pulse separation and spectrometer frequency have been tried. The resulting values of T_1 are consistent at any given temperature.

4.2. Thermometry

The simultaneous measurements of the population in the 3/2–5/2 state and the 5/2–7/2 state are made as follows. The tuning on the coil is set to 390 kHz since the background is quieter than at 260 kHz. The spectrometer

is set at 320 kHz and is operated in the homodyne mode to allow for phase coherence between different traces. A single 32 μsec pulse is used. The Fourier transform of this pulse has frequency components at the position of each of the two lines. The size of the tipping pulse for each transition is only a few degrees. In addition the excitation pulses have roughly the same magnitude for both transitions. The resulting FID signal contains information about both transitions and is recorded as a function of Pt temperature in the course of a demagnetization run. The waiting time between pulses varies from run to run but is never shorter than $5T_1$.

5. RESULTS

5.1. Lineshapes

At temperatures below 8 mK free induction decay signals are visible from the two higher frequency transitions. For the 3/2–5/2 transition the lineshape can be well fitted by a Gaussian with a full width at half maximum of 17 kHz. This corresponds to an FID with a characteristic decay time of 32 ± 1 μsec. The 5/2–7/2 signal is slightly more complicated; it seems to be made up of two Gaussians, one centered at 400 kHz, the second centered at 378 kHz. The decay time of the FID corresponding to the higher frequency line is 25 ± 2 μsec; the corresponding decay time of the lower frequency line is 33 ± 4 μsec. The splitting of the 390 kHz line occurs for a variety of excitation pulses and frequencies. An external magnetic field of 10 Gauss would cause this splitting, but if such a field were present a splitting of the 260 kHz line should have been observed. Furthermore, it would be hard to understand the origin of such a field.

5.2. Relaxation Time Measurements

Figure 4 shows a typical *linear* relaxation plot for the 3/2–5/2 transition at 1 mK. These plots are displayed as ΔM as a function of delay time. The data points are the result of integrating the Fourier transform of one phase of the FID signal over a suitable region.

Two separate regimes for the relaxation are observed, possibly indicating two different relaxation processes. The short time (delays up to 0.1 sec) relaxation is very fast (inset Fig. 4). One unusual feature displayed in this regime is an apparently single exponential relaxation with a time constant that decreases as the temperature is decreased (see Fig. 5). The time scale ranges approximately from 0.1 sec at 8 mK to 0.03 sec at 0.3 mK. In addition there is a small "overshoot" in the recovering magnetization which becomes more prominent at lower temperature. This feature is more prominent in our previous studies of polycrystalline samples[18] where the overshoot of

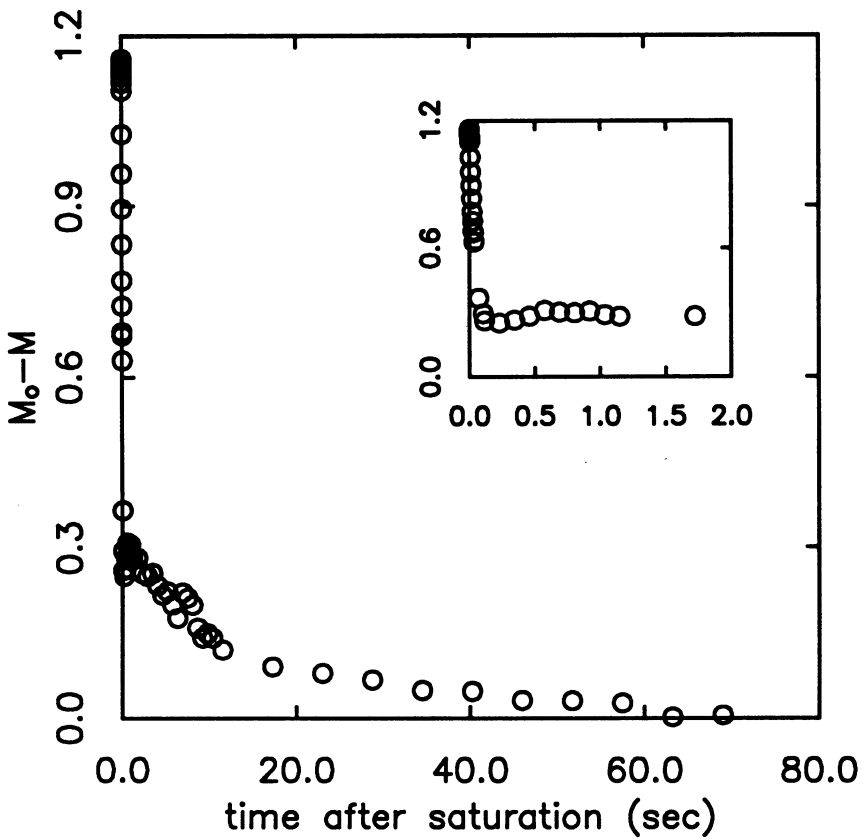

Fig. 4. A typical relaxation curve taken on the single crystal sample at $T = 1$ mK. The inset is a detail of the early time region showing the transition from fast to slow relaxation and the appearance of a very slight minimum.

the initial recovery is more pronounced and there is a minimum in the relaxation curves (see Fig. 6) at a fixed time of 0.1 sec after saturation independent of temperature, over the entire temperature range investigated. One would expect a thermal process to have a temperature dependence. The polycrystalline recovery curve shown in Fig. 6 was taken at the same temperature as the trace from the single crystal shown in Fig. 4. For the single crystals the minimum is still visible at the same time interval although it is not as pronounced. In addition the fits done for the later time relaxation (described below) suggest that the magnetization is left in an unusual state at $t = 0.1$ sec. If we assume that a given transition is saturated at $t = 0$ the populations among the levels redistribute into an "anti-thermal" distribution

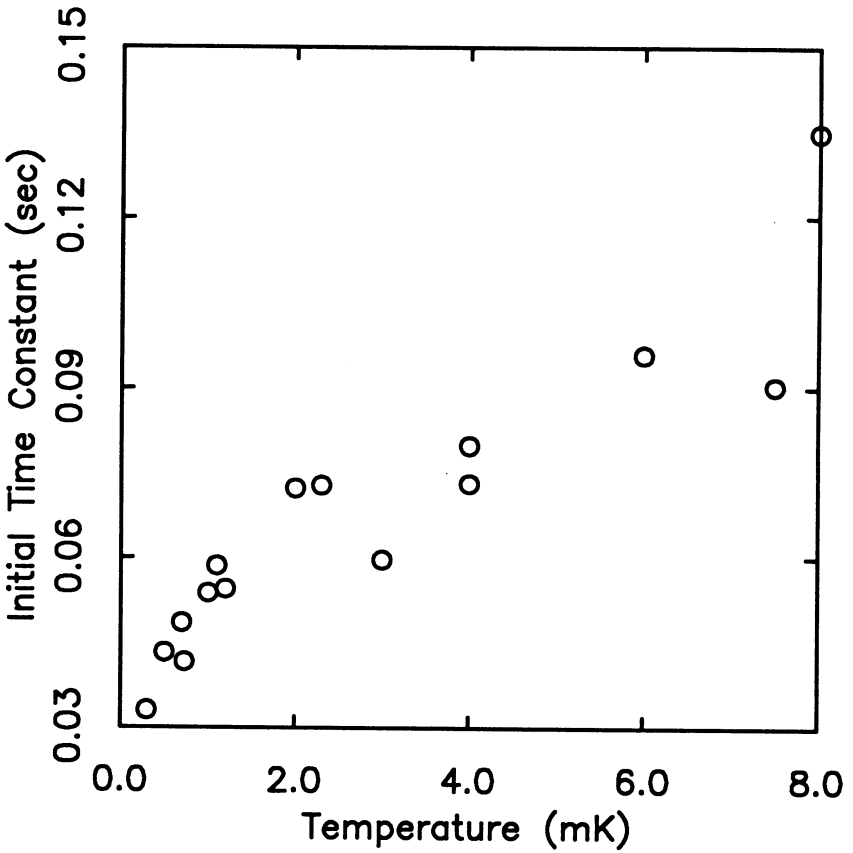

Fig. 5. The data points represent the characteristic time constant of the best fit of a single exponential decay to the initial fast relaxation. The time constant decreases as the temperature decreases.

following this fast relaxation; the population in a higher energy levels appears to increase relative to that of a lower enegy level. The coefficients describing the populations in these states vary smoothly as a function of temperature.

A fast initial relaxation could be caused by a long thermal time constant between the sample electrons and the copper bundle;[27] however, a thermal process should not cause an overshoot in the recovery. Rapid initial relaxation has been observed in systems with magnetic impurities[6,28] although in the case of CuMn the initial relaxation was found to be nonexponential.[28] It is well known[29] that magnetic impurities, especially Fe, have a dramatic effect on the behavior of Sc metal at low temperatures. However, it appears

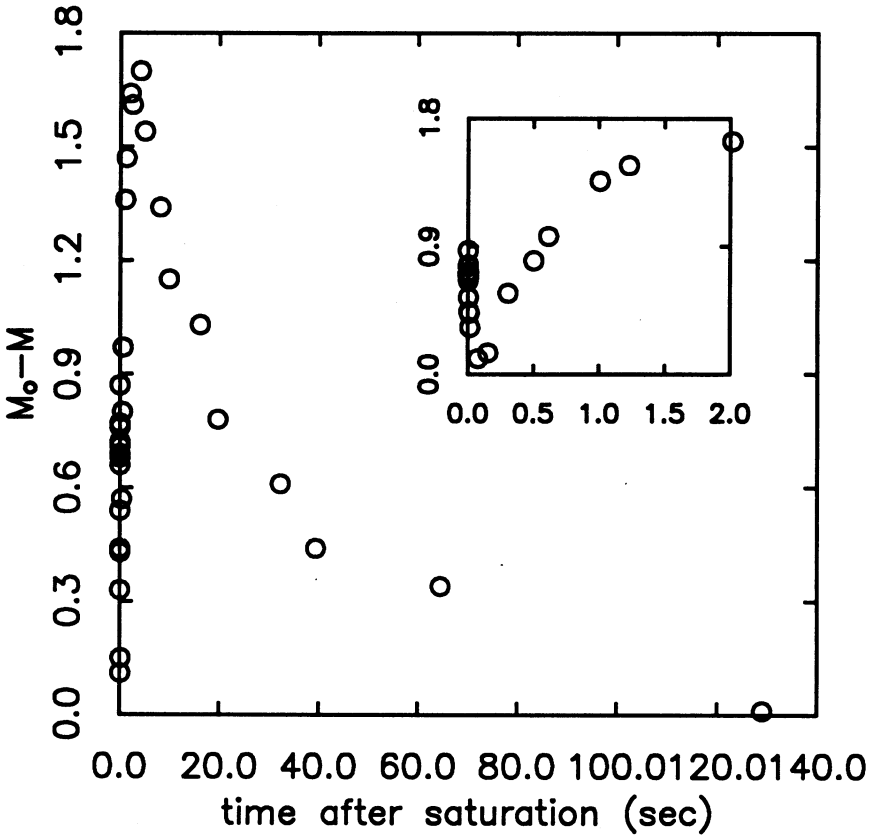

Fig. 6. This relaxation curve was taken on a polycrystalline sample at $T = 1$ mK. The inset again shows the early time region. The minimum is more pronounced than in the case of the single crystal which is shown at the same temperature in Fig. 4.

that low concentrations of Fe, less than 5 ppm, do not alter the behavior of the metal.[30] Our single crystal samples have a 3 ppm Fe impurity concentration. In addition the effect on the relaxation time of the addition of significant amounts of rare earth impurities to Sc has been studied at high field.[31] An enhanced rate of nuclear relaxation was observed. Again our single crystal sample has very low rare earth impurity content (on the order of or less than 1 ppm). One interesting mechanism for enhanced relaxation is discussed in Ref. 32 which involves the coupling of the nuclear spin to the spin of an impurity. Although this mechanism predicts a relaxation rate that increases as the temperature decreases at very low magnetic fields, it is not clear what the expected behavior is at very low temperature.

It is not practical to fit the recovery which occurs between 0.1 sec and 1 sec since this is the cross-over regime between the two different processes. At times longer than 1 sec the decay of the magnetization cannot be adequately fitted by a single exponential. A three-exponential recovery yields a reasonable fit to the data, as expected for the $\Delta m = 1$ relaxation between the nuclear spins and conduction electrons. Data taken at various temperatures have been fitted to Eq. (2) by floating the parameters A, B, C and T_1. Figure 7 shows the result of fitting the data of Fig. 4 to this form. The inset shows the log of the magnetization difference as a function of time after saturation. A single exponential time constant would correspond to a straight line on this plot. The points appear to deviate from such

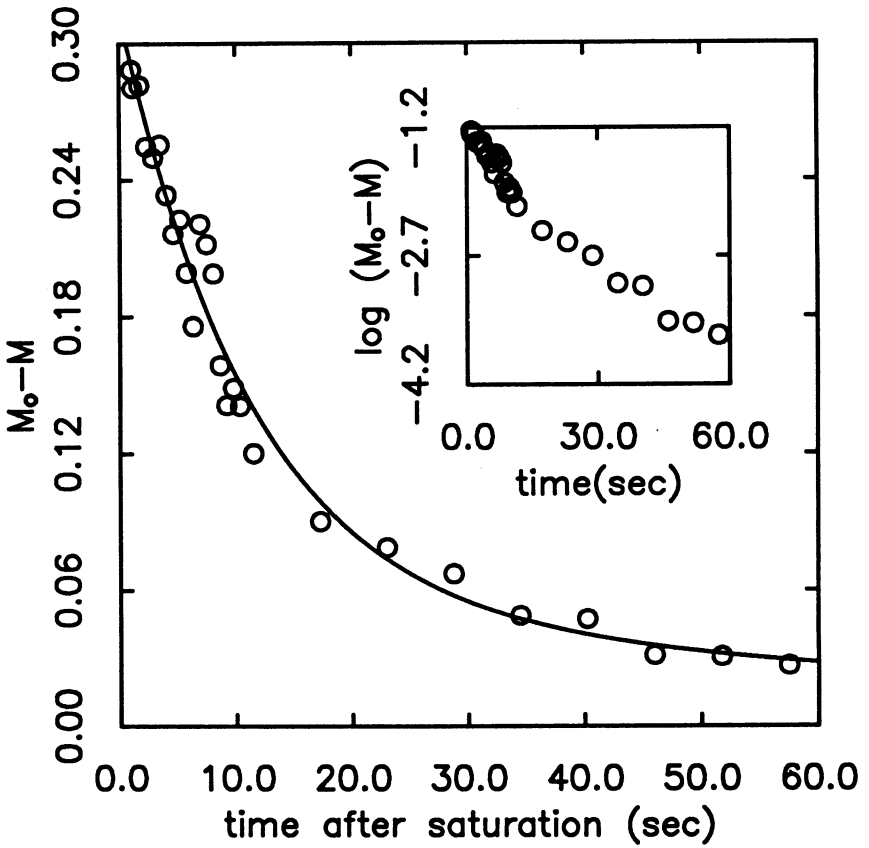

Fig. 7. The solid line represents the best fit of the long time ($t > 1$ sec) data of Fig. 4 to Eq. (2). The time constant, T_1, is extracted from this fit. The inset shows the natural log of magnetization as a function of decay time. A decay characterized by a single time constant would be a straight line on such a plot.

a line. As previously mentioned the values of A B, and C at 1 sec do not correspond to a state in which one set of levels has been saturated, presumably because of the effect of the initial relaxation. The fit to the polycrystalline recovery data is in good agreement with the results from the single crystal. Results for T_1 as a function of temperature are shown in Fig. 8. We find that the Korringa constant for Sc at zero external magnetic field (more precisely at the earth's field which is small compared to the internal fields) is $T_1T = 90 \pm 9$ msec K^{-1} where the quoted error is the statistical error obtained from standard analysis. This value is an order of magnitude shorter

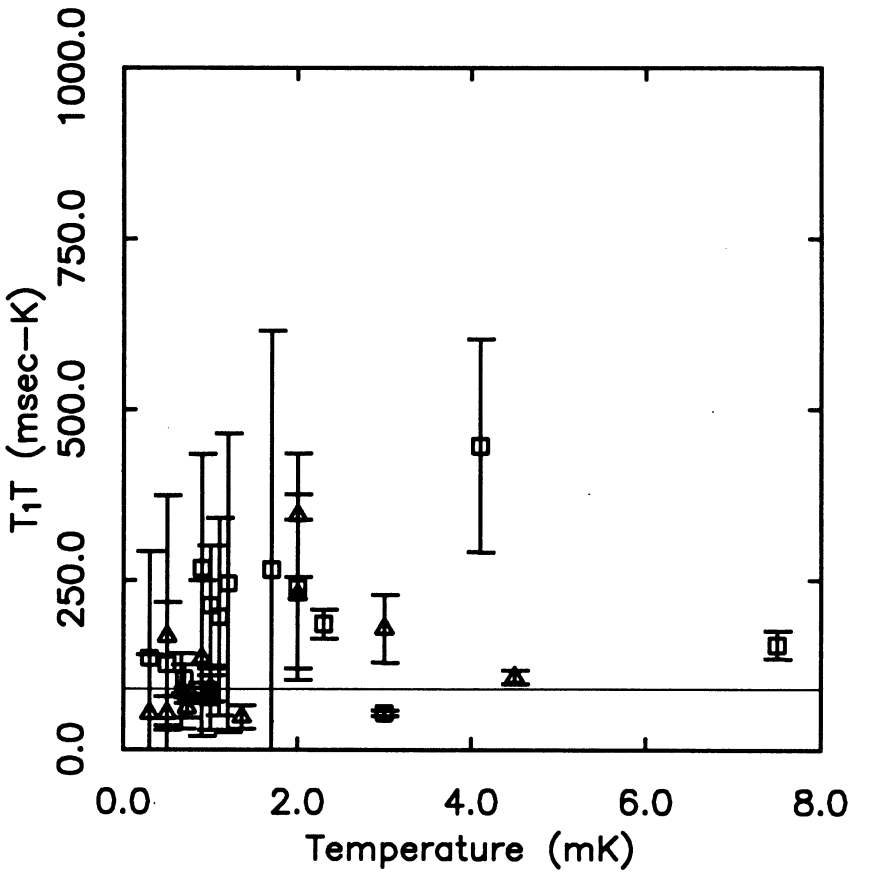

Fig. 8. The open squares represent T_1T from relaxation curves such as the one shown in the previous figure for the 3/2-5/2 transition. The open triangles are data from the 5/2-7/2 transition. In all cases the size of the error bars reflect the quality of the fit to the raw data. The fit to the data to find the Korringa constant was done assuming a standard $1/\sigma^2$ weighting for each data point.

than the values at $B > 0$ and $T > 300$ mK.[2,4] Figure 8 shows data from the two higher frequency transitions. The symbols are described in the figure caption.

We have observed a signal from the 1/2–3/2 transition at about 130 kHz at the lowest temperatures, $T \approx 100\ \mu$K, but the signal is weak.

5.3. Absolute Thermometry and Determination of the Sign of the *E*-Field Gradient

Fourier transforms of FIDs resulting from a pulse used for absolute thermometry are shown in Fig. 9. The x axis is the actual frequency and it

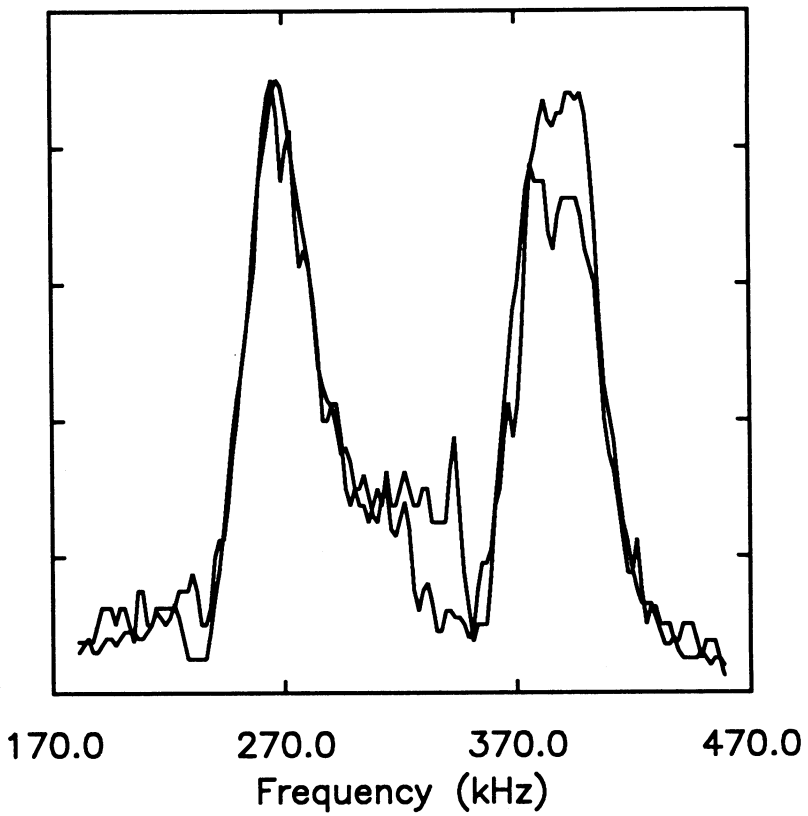

Fig. 9. Two Fourier transform spectra at different temperatures of the response of the spins to a pulse used for thermometry. Both transitions are visible. The trace with less amplitude at 390 kHz was taken at 300 μK; the other was taken at 99 μK. The y axes have been rescaled as explained in the text. The increase in the amplitude of the 390 kHz transition yields information about the sign of the electric field gradient and makes the system useful for absolute thermometry.

is clear that both transitions are resolved. Note that the x axis is rescaled; the spectrometer is set at 320 kHz which explains the additional noise around this frequency on the graph. The two traces shown represent the response of the spins to the same pulse sequence at 300 μK and 99 μK. The y axes have been rescaled so that the height of the 260 kHz peak is the same for both traces. The relative height of the 390 kHz peak is larger for the lower temperature trace. This effect will increase dramatically at even lower temperatures. Figure 10 shows the integrated intensity of the high frequency peak divided by that of the low frequency peak as a function of Pt NMR temperature. We were careful not to include the noise around 320 kHz in

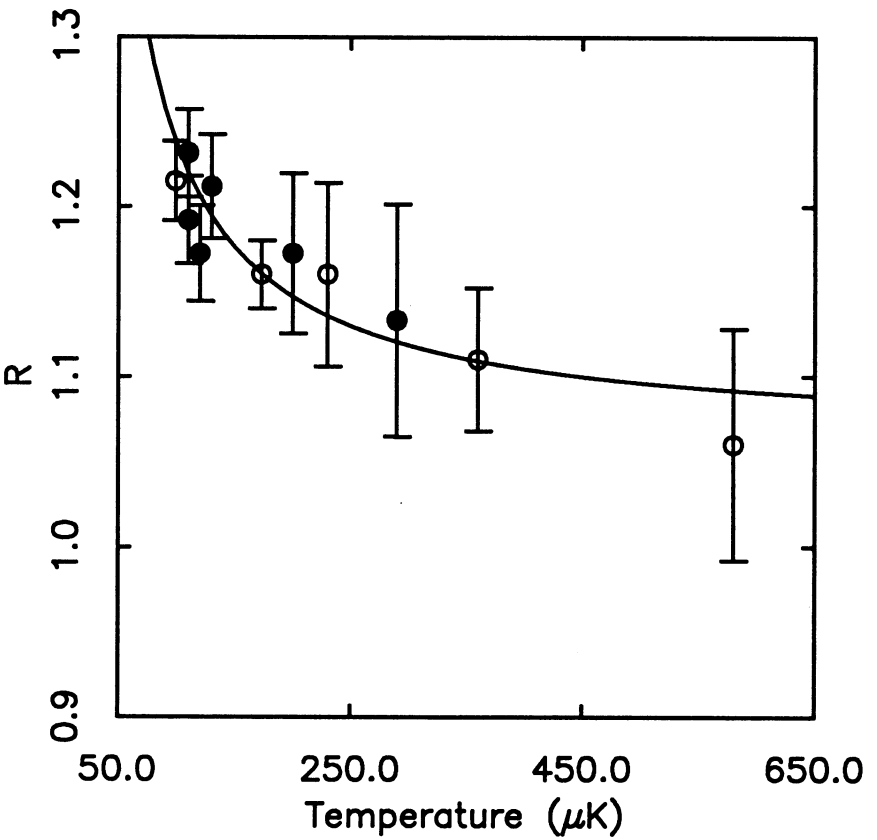

Fig. 10. The data points represent the ratio of the integrated intensity in the high frequency peak to the low frequency peak as a function of temperature. The solid line is the best fit to Eq. (3) through the points. The only free parameter in the fit is an overall multiplicative constant. The open and closed circles represent data taken in two different runs. In some cases signal averaging was employed.

these integrations. The data in this figure were taken in two separate runs, denoted by different symbols. The time between points in both cases was more than 2 h. Although the effect is small it is clear that the intensity in the 5/2-7/2 transition increases relative to that of the 3/2-5/2 transition as the temperature decreases. The line through the data points is a fit to a constant times Eq. (3). (The constant is the high temperature normalizaion previously discussed.) These data and Eq. (3) indicate that the $\pm 7/2$ levels are the ground state of this system. Given that the sign of the electric quadrupole moment of the nucleus is negative, from Eq. (1) it follows that the total field gradient present in the crystal is positive. This measurement provides the first determination of the sign of the total field gradient in Sc. Since the calculated value of the lattice contribution is positive[8] and smaller than the total measured value it follows that the contribution from the conduction electrons is also positive.[10]

6. CONCLUSION AND FUTURE WORK

Quadrupolar systems have several features which makes them useful in the μK regime. First of all they have shorter relaxation times than magnetically split systems of the same order because of their unequally spaced levels. This shorter relaxation time is important for applications such as thermometry. The unequally spaced levels provide a unique opportunity to use these systems as absolute thermometers, which are rare in the μK temperature regime. We have also demonstrated that it is possible to determine the sign of the electric field gradient due to the conduction electrons in Sc.

Quadrupolar systems also provide a unique opportunity to measure the field dependence of the Korringa constants. Although it is possible to measure zero-field relaxation in NMR by field cycling techniques,[33] these measurements are quite easy to make with pure NQR. Since there is evidence of unusual behavior at low fields this is a question of great practical relevance for materials which will eventually be used as demagnetization stages or thermometers. The question of magnetic impurities is also an important one since it is difficult to obtain materials with impurity levels much lower than 10 ppm. If the unusual relaxation effects that we are observing are due to impurities they have a large influence on the behavior of the sample. We plan to repeat these studies in non-zero applied magnetic field. We are also currently pursuing studies in Sc alloys which have larger quadrupolar splittings.

ACKNOWLEDGMENTS

We acknowledge useful discussions with J. H. Ross, Jr. We thank E. Varoquaux for constructing the pre-amplifier and B. Beaudry for preparing

the samples and for many useful discussions about scandium. This work is supported by the NSF through grant number DMR-9109524 and by the Materials Research Division of the NSF through grant number DMR-8818558.

REFERENCES

1. J. Korringa, *Physica* **16**, 601 (1950).
2. A. Narath, *Phys. Rev.* **162**, 310 (1967); T. Asada and K. Terakura, *J. Phys. F* **12**, 1387 (1982).
3. D. E. MacLaughlin, J. D. Williamson, and J. Butterworth, *Phys. Rev. B* **4** 60 (1971).
4. J. W. Ross, F. Y. Fradin, L. L. Isaacs, and D. J. Lam, *Phys. Rev.* **183**, 183 (1969); A. Narath and T. Fromhold Jr., *Phys. Lett.* **25A**, 49 (1967); Y. Masuda, *J. Phys. Soc. Jap.*, **26** 1058 (1969).
5. M. Goldman, *Spin Temperatures and Nuclear Magnetic Resonance in Solids*, Clarendon Press, Oxford (1970).
6. M. T. Hiuku, M. T. Loponen, T. A. Jyrkkio, J. M. Kyynarainen, A. S. Oja, and J. K. Soini, in *Proceedings of the 17th International Conference on Low Temperature Physics* (North-Holland, Amsterdam, 1984), p. 133.
7. K. Gloos, P. Smeibidl, C. Kennedy, A. Singsaas, P. Sekowski, R. M. Mueller, and F. Pobell, *J. Low Temp. Phys.* **73**, 101 (1988).
8. R. G. Barnes, F. Borsa, S. L. Segel, and D. R. Torgeson, *Phys. Rev.* **137**, A1828 (1965).
9. M. H. Cohen and F. Reif in *Solid State Physics*, F. Seitz and D. Turnbull, eds. (Academic Press, New York, 1958), Vol. 5, p. 321; T. P. Das and E. L. Hahn in *Solid State Physics*, F. Seitz and D. Turnbull, eds. (Academic Press, New York, 1958), Suppl. 1, p. 58.
10. G. Fricke, H. Kopfermann, S. Penselin, and K. Schlupmann, *Naturwiss.* **46**, 106 (1959).
11. F. W. de Wette, *Phys. Rev.* **123**, 2070 (1961).
12. T. P. Das and M. Pomerantz, *Phys. Rev.* **123**, 207 (1961).
13. H. Ernst, E. Hagn, E. Zech, and G. Eska, *Phys. Rev. B* **19**, 4460 (1979).
14. Y. Tang, E. D. Adams, K. Uhlig, and D. N. Bittner, *J. Low Temp. Phys.* **60**, 351 (1985).
15. M. Bloom, E. L. Hahn, and B. Herzog, *Phys. Rev.* **97**, 1699 (1955).
16. M. Bloom and R. Norberg, *Phys. Rev.* **93**, 638 (1954); E. L. Hahn and B. Herzog, *Phys. Rev.* **93**, 639 (1954).
17. G. Eska, *J. Low Temp. Phys.* **73**, 207 (1988).
18. L. Pollack, E. N. Smith, R. E. Mihailovich, J. H. Ross, Jr., P. Hakonen, E. Varoquaux, J. M. Parpia, and R. C. Richardson, *Physica B* **165 & 166**, 793 (1990).
19. See references within reference 9.
20. N. S. Sullivan, *Bulletin of Amer. Phys. Soc.* March 1989, p. 736. P. M. Anderson, N. S. Sullivan, M. Rall, and J. P. Brison, *Physica B* **169**, 453 (1991).
21. Oxford Instruments Ltd., Osney Mead, Oxford OX2 0DX, U.K.
22. Ames Labs, Iowa State University, Ames, Iowa 50011-3020.
23. Avantek, 3175 Bowers Ave., Santa Clara, CA 95054; Comlinear Corp., 4800 Wheaton Dr., Fort Collins, CO 80525; EMI filters from Erie Technological Products, Ltd., Trenton, Ontario, Canada—note we used 1233-000 type filters for the low frequency feedthrough application and 1217-000 filters for the transmit and receive feedthrough. They are not shown in the figure due to space constraints. Hewlett-Packard Co., 19310 Pruneridge Ave., Cupertino, CA 95014; Interface Technology, 2100-T East Alsta Ave., Glendora, CA 91740; Merrimac, P.O. Box 986, 41 Farfield Place, West Caldwell, NJ 07007; Mini-Circuits, P.O. Box 166, Brooklyn, NY 11235; North Hills Electronics, 1 Alexander Place, Glen Cove, NY 11542; EG&G Princeton Applied Research, P.O. Box 2565, Princeton, NJ 08543; Tektronix Inc., P.O. Box 500, Beaverton, OR 97077; Wavetek, 5808 Churchman Bypass, Indianapolis, IN 46203.
24. J. Lepaisant, D. Bloyet and E. Varoquaux, *Rev. Sci. Inst.* **55**, 4, 521 (1984).
25. D. Greywall, *Phys. Rev. B* **33**, 7520 (1986).
26. California Fine Wire Sigmund Cohn, Mt. Vernon, NY.

27. B. G. Turrell, G. Eska, N. Masuhara, and E. Schuberth, *J. Low. Temp. Phys.* **70**, 151 (1988).
28. P. Bernier and H. Alloul, *J. Phys. F: Metal Physics* **3**, 869 (1973).
29. T.-W. E. Tsang and K. A. Gschneidner, Jr., *J. Less-Common Metals* **80**, 257 (1981).
30. T.-W. E. Tsang, K. A. Gschneidner, Jr. and F. A. Schmidt, *Proceedings of the 12th Rare Earth Research Conference*, C. E. Lundin, ed. (Denver Research Institute, 1976), Vol. II, p. 847.
31. F. Y. Fradin, *Phys. Rev. B* **5**, 1119 (1972).
32. H. Benoit, P.-G. de Gennes, and D. Silhouette, *Comptes Rendus* **256**, 3841 (1963).
33. A. G. Anderson and A. G. Redfield, *Phys. Rev.* **116**, 583 (1959).